



# Dehydrogenation of cyclohexanol over Cu/Al<sub>2</sub>O<sub>3</sub> catalysts prepared with different precipitating agents



Nilesh P. Tangale, Prashant S. Niphadkar, Shilpa S. Deshpande, Praphulla N. Joshi\*

Catalysis & Inorganic Chemistry Division, CSIR–National Chemical Laboratory, Dr. Homi Bhabha Road, Pashan, Pune 411008, India

## ARTICLE INFO

### Article history:

Received 25 April 2013

Received in revised form 21 July 2013

Accepted 31 July 2013

Available online 18 August 2013

### Keywords:

Cyclohexanol dehydrogenation

Cu/Al<sub>2</sub>O<sub>3</sub>

Precipitating agent

Tetraalkyl ammonium hydroxide

Characterization

## ABSTRACT

Dehydrogenation of cyclohexanol over Cu/Al<sub>2</sub>O<sub>3</sub> catalysts (molar Cu:Al = 1:1) prepared by reduction of mixed oxide precursors synthesized using different precipitating agents viz. potassium carbonate, tetraalkyl ammonium hydroxides (TAAOHs) and urea was investigated. In order to assess the efficacy of TAAOH further, the chain length of tetraalkyl ammonium cations was also varied and the resulted catalysts were evaluated for their catalytic performance. The catalysts were characterized by powder X-ray diffraction, low temperature nitrogen adsorption, temperature programmed desorption of ammonia and UV–visible diffuse reflectance spectroscopy. The dependence of the catalyst performance on the precipitating agent employed during its synthesis has been clearly demonstrated. The use of TAAOH as precipitating agent led to the formation of a catalyst with better catalytic activity than those prepared using potassium carbonate and urea. Further improvement in the catalytic performance was observed when TAAOH with longer alkyl chain ammonium cation was used. The optimum catalyst prepared by reduction of mixed oxide precursor synthesized using tetrapropyl ammonium hydroxide as precipitating agent, showed highest cyclohexanol conversion (81.5%) and cyclohexanone selectivity (79.6%) at 250 °C on account of higher Cu<sup>+</sup>/Cu<sup>0</sup> ratio, well dispersed copper, higher surface area and lower total acidity with higher contribution of sites with moderate strength.

© 2013 Elsevier B.V. All rights reserved.

## 1. Introduction

Cyclohexanone [cyclohexyl ketone, C<sub>6</sub>H<sub>10</sub>O] has gained a great deal of commercial importance due to its high solvent power and reactivity. By virtue of its peculiar properties, it has occupied a special place in various fields such as an industrial solvent for paints and dyes, in pesticides, an activator in oxidation reactions, an intermediate for pharmaceuticals, films, coating, soaps and more importantly, as a raw material for the production of cyclohexanoneoxime, cyclohexanone resins, adipic acid,  $\epsilon$ -caprolactam, nylon-6, etc. The dehydrogenation of cyclohexanol is an industrially important process for the production of cyclohexanone which is endothermic ( $\Delta H = 65$  kJ/mol) and thermodynamically reversible [1,2]. The combined effect of the endothermic nature and the necessity of minimizing the energy usage has stimulated the search for the promising catalyst that can catalyze the reaction at lower temperature (150–300 °C) rather than at higher temperature (350–450 °C) producing cyclohexanone within acceptable range. At high reaction temperature, catalyst such as the ZnO/CaO, has shown 70% conversion and 99% cyclohexanone selectivity [3]. Under milder conditions, various binary and ternary metal oxide catalyst systems such as CuCr<sub>2</sub>O<sub>4</sub> [1], Cu–Al<sub>2</sub>O<sub>3</sub> [4–7],

Cu–ZnO–Al<sub>2</sub>O<sub>3</sub> [8], Rh–Cu/Al<sub>2</sub>O<sub>3</sub> [9], Cu/SiO<sub>2</sub> [10–12], Cu/Fe/SiO<sub>2</sub> [13], Cu–Zn/SiO<sub>2</sub> [14], Co– $\gamma$ -Al<sub>2</sub>O<sub>3</sub> [15], V<sub>2</sub>O<sub>5</sub>–MoO<sub>3</sub>–M<sub>2</sub>O (M = Na, K, Cs) [16], Cu–Mg/Zn–Al [17,18], CuNi–CeO<sub>2</sub> [19],  $\gamma$ -Al<sub>2</sub>O<sub>3</sub>/ $\alpha$ -Al<sub>2</sub>O<sub>3</sub> [20], Fe–TiMCM-41 [21,22], Cu–Cr–Mg–Al [23], etc. have been reported as an active catalysts. Depending upon the catalyst characteristics and reaction conditions, besides the formation of the desired cyclohexanone product, other by-products such as cyclohexene, phenol, cracked and condensed products are also formed due to dehydrogenation, dehydration and aromatization of cyclohexanol and other side reactions [1,14]. As a result of encouraging results exhibited by Cu-based catalysts at low temperature, one of the several attempts made to enhance the cyclohexanol conversion and cyclohexanone selectivity was the use of catalysts with higher Cu content. Among three active commercial catalysts with Cu = 24, 26 and 65 wt%, the catalyst with 26 wt% Cu has shown higher activity on account of higher dispersion and smaller Cu crystallite size, whereas at 290 °C, the catalyst containing 65 wt% Cu showed about 70% cyclohexanone yield with lower WHSV [1]. These catalysts showed a high stability even at very high time on stream [2]. The possible cause/s for the drop in the initial activity were identified as poisoning, coking and sintering, solid phase transformation, etc. [2]. The combined results of rate measurements and IR spectroscopic studies on Cu–Zn–Al (Cu loading 15 at.%) and Cu–Mg (Cu loading 52 at.%) catalysts showed that, the dehydrogenation of cyclohexanol over Cu<sup>+</sup> proceeds through nondissociative cyclohexanol adsorption with subsequent formation of cyclohexanol

\* Corresponding author. Tel.: +91 20 25902457; fax: +91 20 25902633.

E-mail address: [pn.joshi@ncl.res.in](mailto:pn.joshi@ncl.res.in) (P.N. Joshi).

alcoholate, whereas cyclohexanol adsorption on Cu<sup>0</sup> is dissociative and proceeds via formation of cyclohexanol alcoholate and phenolate species [18]. Cu/SiO<sub>2</sub> catalyst with copper content as high as 50 wt%, prepared by precipitation at pH > 9 using sodium carbonate as precipitating agent showed 74.7% cyclohexanone yield at 300 °C [11]. The selectivity to cyclohexanone may also be governed by the acidity of support metal oxide [10,11,24].

The chemical kinetics and mechanism of the reaction showed that, the two kinds of copper active sites are present on the catalyst viz. monovalent copper and metallic copper. The metallic copper is responsible for the phenol formation and selectivity of cyclohexanone while monovalent copper is responsible for formation of cyclohexanone only [17]. At low temperature, catalytic performance of copper-based catalysts primarily depends on the presence of metallic copper and monovalent active sites [17]; the acid–base nature of catalyst [5]; and the size, population and dispersion of the Cu species [1]. The activity and stability of the Cu containing catalyst mostly depend on the preparation method and the parameters employed in the particular method [7]. Several methods such as, chemisorption hydrolysis [5], precipitation [7,8,11,17,18], ion exchange [12], impregnation [12–14], electroless plating [6], sol–gel [25], etc. were reported for preparation of copper-based catalysts. Among these methods, co-precipitation method is the better choice for the controlled preparation of binary and ternary metal oxide catalyst systems from simplicity and scale up point of view. By this method, one can also minimize the deposition of non-uniform layered copper which are very susceptible to sintering and hence in turn catalyst life and activity. In simultaneous co-precipitation method, it is very important to select precipitating agent judiciously as it plays a crucial role in the controlling the size and dispersion of the copper. Various precipitating agents such as aqueous solutions of Na<sub>2</sub>CO<sub>3</sub>, K<sub>2</sub>CO<sub>3</sub>, (NH<sub>4</sub>)<sub>2</sub>CO<sub>3</sub>, NaOH, KOH, NH<sub>4</sub>OH and urea were commonly used to prepare the Cu/Al<sub>2</sub>O<sub>3</sub> catalysts. Although, the tetraalkylammonium hydroxides (TAAOH) were used in synthesis of zeolite or zeolite-like materials [26–28], stabilization of metal colloids [29], preparation of nanocrystalline yttrium oxide [30], spinel cobalt ferrite [31] and nanosized titania powder [32], etc. until now, as per our knowledge, there are no reports on use of TAAOHs as precipitating agents for the preparation of binary/ternary metal oxide catalyst systems with a view to maximize the yield of cyclohexanone by cyclohexanol dehydrogenation.

The aim of work is to investigate the performance of Cu/Al<sub>2</sub>O<sub>3</sub> catalysts (molar Cu:Al = 1:1) prepared by reduction of mixed oxide precursors synthesized using different precipitating agents viz. potassium carbonate, TAAOH and urea in dehydrogenation of cyclohexanol. In view of maximizing the cyclohexanone yield, further assessment of the efficacy of TAAOH was examined by varying the chain length of tetraalkyl ammonium cations. All the catalysts were characterized by powder X-ray diffraction, low temperature nitrogen adsorption, temperature programmed desorption of ammonia and UV–visible diffuse reflectance spectroscopy. Finally, results of the cyclohexanol dehydrogenation to cyclohexanone over Cu/Al<sub>2</sub>O<sub>3</sub> catalysts at reaction condition of 250 °C were discussed and presented in this paper.

## 2. Experimental

### 2.1. Materials

Aluminum nitrate nonahydrate (98%), copper nitrate trihydrate (99.5%), cyclohexanol (99%) were procured from Loba Chemie, Mumbai, India. Potassium carbonate (99.5%) and urea (99.5%) were procured from Thomas Baker and Qualigens respectively. Aqueous

(20%) solutions of tetramethyl ammonium hydroxide (TMAOH), tetraethyl ammonium hydroxide (TEAOH), tetrapropyl ammonium hydroxide (TPAOH) were purchased from V.P. Chemicals, Pune, India.

### 2.2. Catalyst preparation

Cu/Al<sub>2</sub>O<sub>3</sub> catalysts (molar Cu:Al = 1:1) were prepared by reduction of mixed oxide precursors. These precursors were synthesized by simultaneous co-precipitation method similar to described elsewhere [33]. Aqueous solutions of potassium carbonate, TMAOH, TEAOH and TPAOH were used separately as precipitating agents. Typically, solution A was prepared by dissolving 9.1 g of Cu(NO<sub>3</sub>)<sub>2</sub>·3H<sub>2</sub>O in 250 ml deionized water followed by the addition of 14.07 g of Al(NO<sub>3</sub>)<sub>3</sub>·9H<sub>2</sub>O. The solution B was prepared by dissolving 20.73 g of anhydrous K<sub>2</sub>CO<sub>3</sub> in 250 ml deionized water. Solutions A and B were simultaneously added with constant rate at room temperature under vigorous stirring. The final pH of solution was adjusted to 8.5. The stirring was further continued for 5 h at room temperature. The precipitate was then recovered by filtration, washed thoroughly till effluent showed no potassium and then dried at 100 °C for 12 h. The dried powder was ground to fine powder and then calcined at 400 °C for 3 h. The sample was designated as CAR. By following the identical procedure, mixed oxide precursors were prepared using different precipitating agents viz. aqueous solutions of TMAOH, TEAOH and TPAOH. The resultant samples were designated as TMA, TEA and TPA respectively.

For catalytic testing purpose, a catalyst designated as Alumina was prepared by following the identical procedure as described above except use of Cu(NO<sub>3</sub>)<sub>2</sub>·3H<sub>2</sub>O.

Another mixed oxide precursor was prepared by following homogeneous precipitation method using urea similar to described elsewhere [4]. In a typical procedure, a solution was prepared by dissolving 9.1 g of Cu(NO<sub>3</sub>)<sub>2</sub>·3H<sub>2</sub>O in 250 ml deionized water followed by the addition of 14.07 g of Al(NO<sub>3</sub>)<sub>3</sub>·9H<sub>2</sub>O. To this solution, an aqueous solution containing required amount of urea was added with constant stirring. This homogeneous solution was heated at 92 ± 3 °C till pH becomes 7.5. The precipitate was recovered by filtration, washed thoroughly with de-ionized water, dried at 100 °C for 12 h and finally calcined at 400 °C for 3 h. The sample was designated as URE.

### 2.3. Characterization

The phase identification, relative crystallinity and an estimation of the crystallite sizes (by applying Debye–Scherrer equation) were carried out by powder X-ray diffraction (XRD) patterns recorded on a P Analytical PXRD system (Model XPert-PRO-1712) using Ni filtered Cu K $\alpha$  radiation ( $\lambda = 0.154$  nm). For elucidating the nature of copper species in the samples, a diffuse reflectance UV–vis (DRUV–vis) spectrum was recorded on a Perkin–Elmer Lambda 6 spectrometer (Lambda 650) using BaSO<sub>4</sub> as a reference. BET surface areas were measured by N<sub>2</sub> adsorption measurements at –196 °C using Quanta Chrome CHEMBET 3000 instrument. The acidity and acidic strength of sites were measured by NH<sub>3</sub>–temperature programmed desorption using Micromeritics ChemiSorb (2720, USA) equipped with thermal conductivity detector. The samples were degassed at 200 °C in He (25 cm<sup>3</sup> min<sup>–1</sup>) for 1 h prior to the measurement. Then, the temperature was decreased to 35 °C and NH<sub>3</sub> was allowed to adsorb by exposing the gas stream containing 10% NH<sub>3</sub> in He for 1 h. It was then flushed with He for another 1 h. The NH<sub>3</sub> desorption was carried out in He flow (25 cm<sup>3</sup> min<sup>–1</sup>) by increasing the temperature up to 750 °C with the heating rate of 10 °C min<sup>–1</sup>.

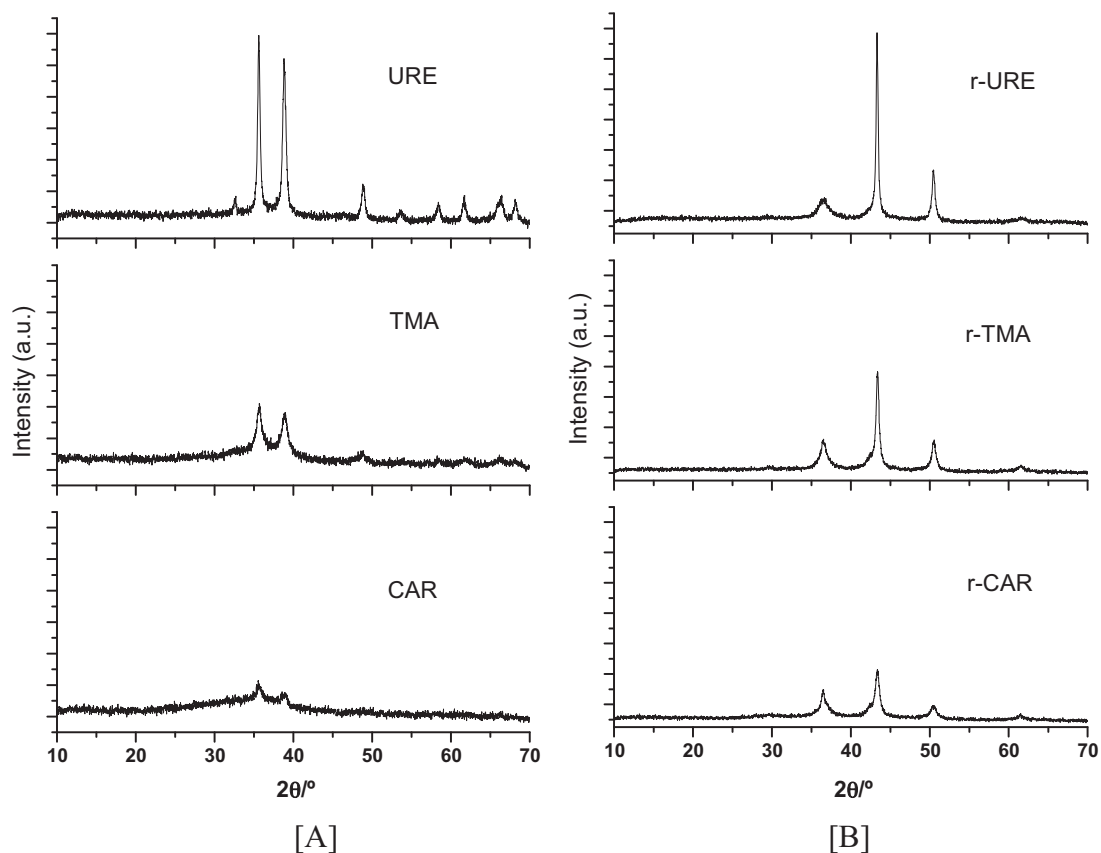


Fig. 1. X-ray diffraction patterns of (A) URE, TMA, CAR and (B) r-URE, r-TMA, r-CAR.

#### 2.4. Catalytic activity

The dehydrogenation of cyclohexanol over  $\text{Cu}/\text{Al}_2\text{O}_3$  catalysts (molar  $\text{Cu}:\text{Al}=1:1$ ) prepared by reduction of mixed oxide precursors synthesized using different precipitating agents was carried out in a continuous, down-flow, fixed bed reactor (SS316, 40 cm length, 2 cm I.D.) at atmospheric pressure. In a reactor, the reduced catalyst (3.0 g, self-bound granules with 20–40 mesh size) was sandwiched at the center by inert ceramic beads. The reactor was heated to the required temperature with an electrical tubular furnace having digital temperature controller cum indicator. The mixed oxide precursor was reduced in situ in a  $\text{H}_2$  flow of  $55 \text{ cm}^3 \text{ min}^{-1}$  at  $250^\circ\text{C}$  for 8 h. The cyclohexanol was fed to the reactor with weight hour space velocity (WHSV) ranging from 3.0 to  $10.0 \text{ h}^{-1}$  with nitrogen ( $50 \text{ cm}^3 \text{ min}^{-1}$ ). The product was collected after 1 h and analyzed by gas chromatography (Shimadzu, HP 5890A) using a flame ionization detector (FID) and carbowax column (30 m length, 0.53 mm I.D. and  $1 \mu\text{m}$  film thickness). Quantification of various products was accomplished using response factors of typical standard mixtures. The liquid mass balance was  $98 \pm 2\%$ . Based on the product distribution pattern, the cyclohexanol conversion and the selectivity to the products such as, cyclohexanone, phenol, and cyclohexene were calculated.

### 3. Results and discussion

#### 3.1. Characterization of CAR, URE and TMA

Fig. 1A shows the powder X-ray diffraction patterns of CAR, URE and TMA. All the samples have shown the presence of the characteristic peaks  $\text{CuO}$  phase (JCPDS File no. 65-2309) [33–35] of which most prominent peaks appeared at  $35.6^\circ$  and  $38.85^\circ$ . The intensity

and full width at half maximum (FWHM) of these peaks were found to be weaker and broader in case of CAR compared to TMA. Moreover, the most intense and narrow peaks were observed in case of URE. The degree of crystallinity and the magnitude of crystallite size of  $\text{CuO}$  were found to follow the trend as:  $\text{CAR} < \text{TMA} < \text{URE}$ . The crystallite size and intensity of the  $\text{CuO}$  peaks can be taken as an indirect measure, at least qualitatively, to analyze the copper dispersion [1,36,37]. Thus, considering the trend observed in the degree of crystallinity and the crystallite size, the copper dispersion in samples followed the trend as:  $\text{CAR} > \text{TMA} > \text{URE}$ . This can be partly explained on the basis of the type of the anionic species that were made available by the precipitating agent during precipitation process. In case of potassium carbonate precipitating agent, the carbonate species generated during precipitation process are likely to form molecular precursors such as amorphous/crystalline forms of  $\text{Cu}_2(\text{OH})_2\text{CO}_3$ , along with  $\text{Cu}(\text{OH})_2$  and  $\text{CuO}$  phases [41]. Whereas, in case of other two precipitating agents, formation of copper hydroxides and/or  $\text{Cu}_2(\text{OH})_3\text{NO}_3$  [4] which formed the basis for the formation of more crystalline  $\text{CuO}$  phase after calcination. The extent of interdiffusion of copper and aluminum during the calcination may also be responsible for the variation in the crystallinity of  $\text{CuO}$  with variation in type of the precipitating agent used. Compared to other two samples, the larger crystallite size of  $\text{CuO}$  in URE may be associated with higher rate of nucleation of primary particles and enhanced acceleration in the growth of primary particles probably due to the strong interaction of copper with support oxide [30]. Further, the reduction in crystallite size of  $\text{CuO}$  in TMA might be associated with the suppression of the growth of precipitate particle size by promoting the nucleation of new particle during precipitation [30]. All the three samples showed no peaks due to alumina indicating the presence of amorphous alumina. Moreover, no XRD visible contribution of phase/s such as

**Table 1**  
BET surface area, crystallite size, Cu<sup>+</sup>/Cu<sup>0</sup> ratio and acidic site distribution of catalysts prepared by reduction of mixed oxide precursors synthesized using different precipitating agents.

Catalyst	BET specific surface area (m <sup>2</sup> g <sup>-1</sup> )	Crystallite size (nm)		Cu <sup>+</sup> /Cu <sup>0</sup>	Total acidity (mmol g <sup>-1</sup> )	Acid site distribution (%)		
		Cu <sub>2</sub> O ( <i>d</i> = 0.24635)	Cu <sup>0</sup> ( <i>d</i> = 0.20868)			Weak	Moderate	Strong
r-CAR	70	14.3	11.9	0.51	0.184	20.5	64.3	15.2
r-URE	53	8.8	26.9	0.55	0.173	21.9	71.7	6.4
r-TMA	102	11.7	17.6	0.42	0.163	20.0	73.4	6.6
r-TEA	104	11.4	15.9	0.45	0.161	19.3	76.1	4.6
r-TPA	139	9.4	13.3	0.56	0.158	17.1	78.4	4.5

Cu<sub>2</sub>O, CuAl<sub>2</sub>O<sub>4</sub>, CuAlO<sub>2</sub>, CuAl<sub>4</sub>O<sub>7</sub>, etc. was observed in all the three samples.

After reducing CAR, TMA and URE samples in a H<sub>2</sub> flow (55 cm<sup>3</sup> min<sup>-1</sup>) at 250 °C for 8 h, they were designated as r-CAR, r-TMA and r-URE, respectively. The XRD patterns of all these reduced samples are shown in Fig. 1B. All the samples have exhibited characteristic peaks due to Cu<sub>2</sub>O phase (JCPDS File no.78-2076) and metallic copper (JCPDS File no. 85-1326) [37] at the cost of CuO phase. In all the samples, there is complete disappearance of CuO phase after reduction. The most prominent peaks of Cu<sub>2</sub>O phase were appeared at 36.45° and 43.32° whereas of metallic copper were indexed at 43.32° and 50.44° [33]. The trend observed in the degree of crystallinity and the magnitude of crystallite size of Cu<sub>2</sub>O and metallic copper were found to follow the similar trend as CuO phase as: CAR < TMA < URE. Although, the intensity of the peaks of Cu<sub>2</sub>O and metallic copper were reported to increase with increase in the copper content [38,39], in present studies, it may be attributed to the variation in the precipitating agent as there is no variation made in the copper content. Irrespective of the precipitating agent used, it is likely that, during reduction process, the sequential reduction of CuO to Cu<sub>2</sub>O cubical phase occurs first as stable intermediate and then to metallic copper [33]. The crystallite size of metallic copper was estimated by Debye–Scherrer equation and the values were summarized in Table 1.

In cyclohexanol dehydrogenation to cyclohexanone reaction, monovalent copper and metallic copper are the two kinds of active sites which are revealed as selective and non-selective sites respectively [17]. Therefore, an assessment of XRD patterns of r-CAR, r-TMA and r-URE was carried out to estimate the relative proportions of XRD visible Cu<sub>2</sub>O and metallic copper phases. The ratio between the integrated area under the peaks associated with the Cu<sub>2</sub>O and the integrated area under the peaks associated with the metallic copper was taken as a measure for the qualitative analysis and these values are provided in Table 1 as Cu<sup>+</sup>/Cu<sup>0</sup>. The BET surface areas of r-URE, r-TMA and r-CAR are also included in Table 1. It is clearly evident that, the trend observed in Cu<sup>0</sup> crystallite size was as: r-CAR < r-TMA < r-URE whereas in the BET surface area, it was as: r-URE < r-CAR < r-TMA. Interestingly, the r-URE sample has shown lower surface area in spite of having larger crystallite size. Similarly, r-TMA has shown higher surface area than r-CAR despite the fact that it has larger crystallite size compared to r-CAR. Such mismatch may be attributed to the differences in the origin of the target material. The estimation of crystallite sizes was done using metallic copper phase whereas the target material for evaluation of BET surface area was the Cu/Al<sub>2</sub>O<sub>3</sub> composite phase. Probably, larger crystallite size of Cu<sup>0</sup> in r-URE may also be responsible for the formation of bigger particles via aggregation leading to decrease in BET surface area. Although the samples were reduced under the identical conditions, Cu<sup>+</sup>/Cu<sup>0</sup> were found to vary with the variation in precipitating agent (Table 1). Thus, there exists a dependence of relative proportions of XRD visible selective and non-selective catalytic active sites on the precipitating agent. In this regard, compared to XRD visible metallic copper (non-selective) sites, the population of monovalent copper (selective) sites was

found to follow the trend as: r-URE > r-CAR > r-TMA. Assuming that, the differences in the chemical environment and coordination of copper species present in pre-reduced samples may be the one of the reasons for showing such trend, further probing experiments were conducted using DRUV–vis spectroscopy.

The deconvoluted DRUV–vis spectra of CAR, URE and TMA are shown in Fig. 2. Upon deconvolution, three peaks were emerged and their area percentages are provided in Table 2. As can be seen from the deconvoluted spectra of all the three samples that, (1) the first band maximum was observed at about 280 nm, (2) the second maximum was observed in the range of 350–450 nm, and (3) the third maximum observed at about 650 nm. These bands can be ascribed to the charge transfer between mononuclear Cu<sup>2+</sup> ion and oxygen, the charge transfer between Cu<sup>2+</sup> cluster and oxygen in [Cu–O–Cu]<sub>n</sub> cluster-like species and the d–d transition of Cu with an octahedral environment in CuO [37,40,41], respectively. These assignments and the corresponding values in Table 2 indicated that, the precipitating agents play a prominent role in the distribution of copper species as isolated Cu<sup>2+</sup> cations, oligonuclear [Cu–O–Cu]<sub>n</sub> species and crystalline CuO. The heterogeneous distribution and population of readily reducible copper ions and copper cluster species might be responsible for governing the ratio of metallic copper (non-selective) to the monovalent copper (selective) sites after their reduction.

The nature of acidic sites in r-URE, r-CAR and r-TMA were evaluated by temperature programmed desorption of ammonia measurements. The profiles which were obtained in the present studies are shown in Fig. 3 and acid site distribution depending on their strengths is tabulated in Table 1. It can be seen that, three prominent desorption zones appeared at lower temperature (<200 °C), in the temperature range (200–500 °C), in the higher temperature (500–750 °C) regions. The origin of these zones can be assigned to presence of weak, moderate and strong acidic sites, respectively [13]. The trend in % contribution due to weak acidic sites was found to follow the trend as: r-URE > r-CAR > r-TMA. Moreover, the trend observed in % contribution due to intermediate acidic sites was as: r-TMA > r-URE > r-CAR. Further, the trend observed in % contribution due to strong acidic sites was as: r-CAR > r-TMA > r-URE. The higher acidity of the catalyst plays an important role in favoring the selectivity of cyclohexene by dehydrogenation of cyclohexanol [10,11,24]. It can be seen from Table 1 that, r-CAR and r-URE catalysts possess higher total acidity as compared to the catalyst r-TMA.

**Table 2**  
Variations in percentages of isolated Cu<sup>2+</sup> cations, oligonuclear [Cu–O–Cu]<sub>n</sub> species and crystalline CuO as a function of precipitating agents.

Catalyst	Isolated Cu <sup>2+</sup>	[Cu–O–Cu] <sub>n</sub>	CuO
URE	21	60	19
CAR	27	57	16
TMA	23	59	18
TEA	18	62	20
TPA	17	64	19

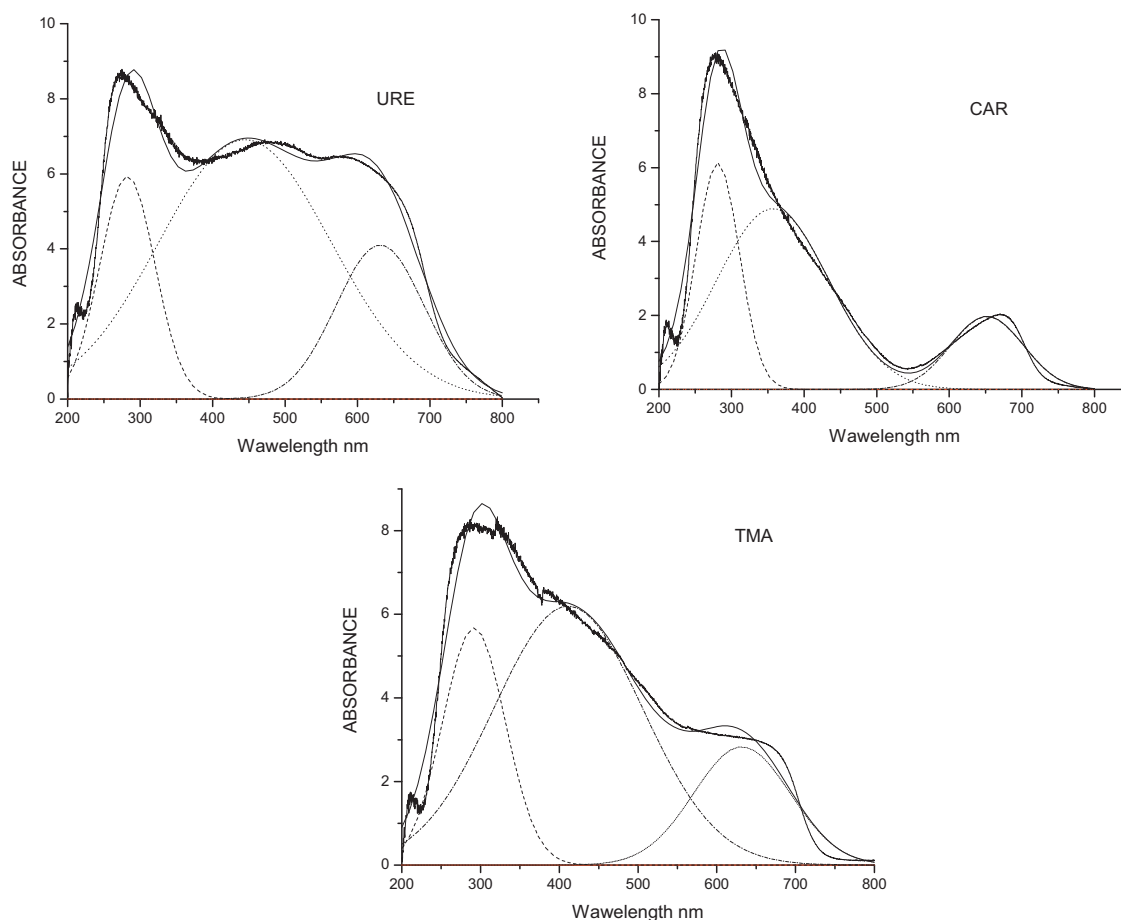


Fig. 2. DRUV-vis spectra of URE, TMA and CAR.

### 3.2. Characterization and comparison of TEA and TPA with TMA

In order to maximize the conversion of cyclohexanol in dehydration of cyclohexanol reaction, attempts were made to prepare mixed oxide precursors using TAAOH having longer alkyl chain ammonium cations. The powder X-ray diffraction patterns of TEA and TPA were shown along with TMA for comparison purpose in

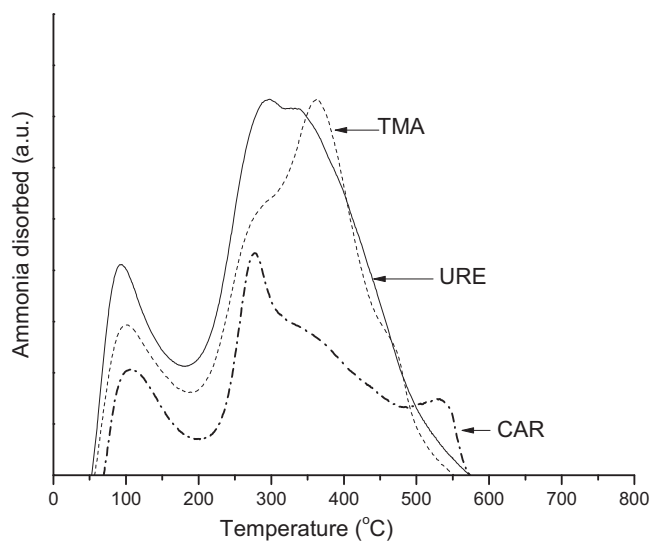


Fig. 3.  $\text{NH}_3$ -TPD profiles r-URE, r-TMA and r-CAR.

Fig. 4A. The intensity of CuO peaks were found to increase with the decrease in chain length of tetraalkyl ammonium cation. The lower intensities and higher FWHM of peaks for CuO in TPA sample indicates high dispersion of smaller CuO species than TMA and TEA samples [1,36,37]. Similarly, the powder X-ray diffraction patterns of r-TEA and r-TPA were shown along with r-TMA for comparison purpose in Fig. 4B. The intensity and width of the diffraction lines of metallic copper were found to increase with the decrease in chain length of tetraalkyl ammonium cation. The ratio between the integrated area under the peaks associated to the  $\text{Cu}_2\text{O}$  and the integrated area under the peaks associated to the metallic copper ( $\text{Cu}^+/\text{Cu}^0$ ) were estimated and provided in Table 1. The BET surface areas of r-TEA and r-TPA are also included in Table 1. It is clearly evident from the Table 1 that, longer the alkyl chain ammonium cation, smaller the crystallite size of the catalyst. The reverse trend was observed in case of BET surface area. The r-TPA has shown the higher BET surface area and smaller crystallite size among all the three samples. This can be explained partly on the basis of longer chain length of tetrapropyl ammonium cation which might be responsible for the reduction in collision rate during precipitation and suppression of particle growth rate [32]. Longer alkyl chain ammonium cation seems to be operative in the increasing the relative distance between precipitated copper species-hydroxide entity which results in the increase in the nucleation growth. The extent of suppression in the copper agglomeration was found to follow the trend as: r-TMA > r-TEA > r-TPA.

Although, the samples were reduced under the identical conditions,  $\text{Cu}^+/\text{Cu}^0$  were found to vary with the variation in chain length of tetraalkyl ammonium cation. The  $\text{Cu}^+/\text{Cu}^0$  ratio (Table 1) was found to increase with increase in the chain length of tetraalkyl

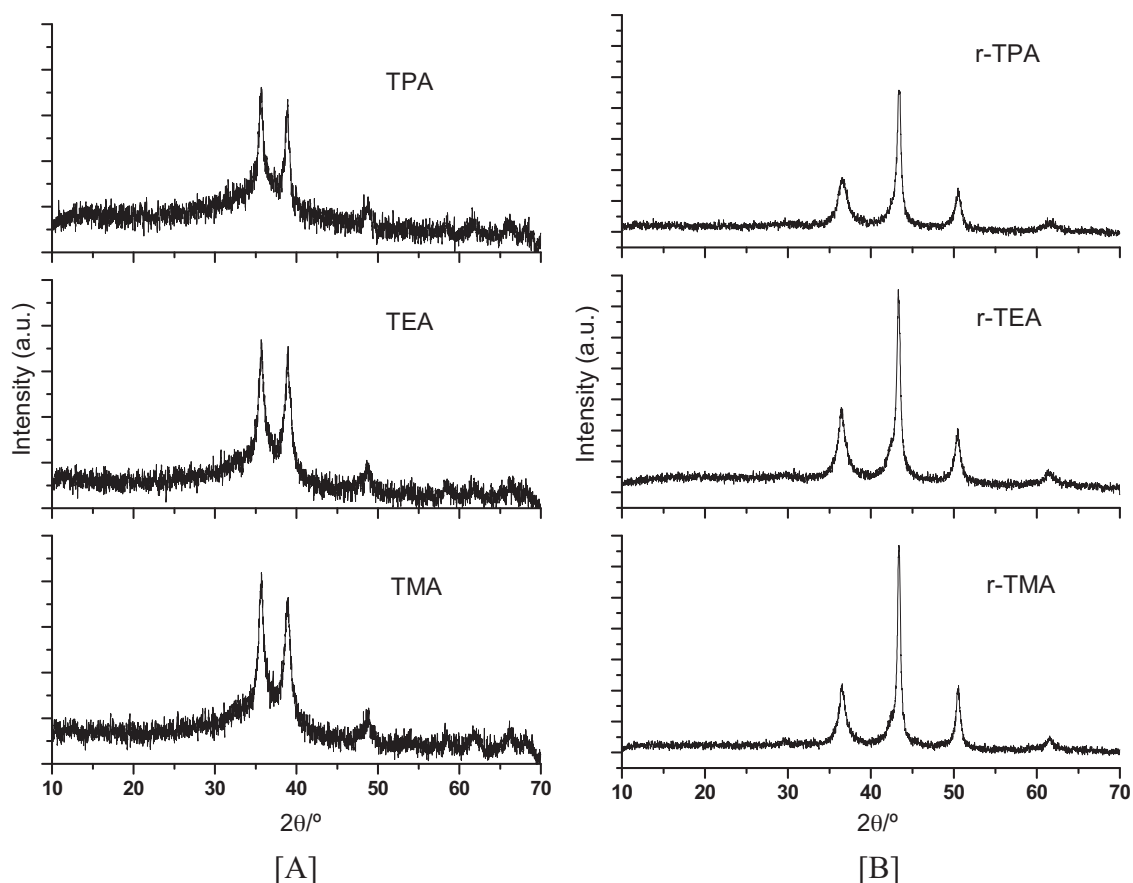


Fig. 4. X-ray diffraction patterns of (A) TMA, TEA, TPA and (B) r-TMA, r-TEA, r-TPA.

ammonium cation and followed the trend as:  $r\text{-TMA} < r\text{-TEA} < r\text{-TPA}$ . Thus, longer the chain length of tetraalkyl ammonium cation, higher is the population of  $\text{Cu}^+$  as compared to  $\text{Cu}^0$  that are XRD visible.

DRUV–vis absorption spectra of TMA, TEA and TPA were recorded to understand the nature of Cu species in catalyst as shown in Fig. 5. Similar to TMA, TEA and TPA have exhibited the similar patterns except the changes in the area percentages of deconvoluted peaks. The distribution of copper species of all the catalysts is summarized in Table 2. It can be clearly seen from the table that, as the chain length of the tetraalkyl ammonium cation increases, there is a decrease in the percentage of mononuclear  $\text{Cu}^{2+}$  species accompanied by the increase in the oligomeric  $[\text{Cu-O-Cu}]_n$  species. However, the amount of  $\text{CuO}$  species in all the samples remained unaltered irrespective of the chain length of organocation.

Further attempts were made to study the effect of chain length in tetraalkyl ammonium cation on the acidity of catalysts by establishing the  $\text{NH}_3$ -temperature programmed desorption of ammonia profiles. The profiles of r-TMA, r-TEA and r-TPA (Fig. 6) showed prominent peaks assigned to weak acidic sites ( $<200^\circ\text{C}$ ), moderate acidic sites ( $200\text{--}500^\circ\text{C}$ ) and strong acidic sites ( $500\text{--}700^\circ\text{C}$ ). The total acidity expressed as millimoles of ammonia desorbed per g of catalyst and % distribution of the acid sites are provided in Table 1. The total acidity was found to decrease with the increase in the chain length in tetraalkyl ammonium cations. The contribution due to weak and strong acid sites in all the catalysts was found to decrease with the increase in the chain length of tetraalkyl ammonium cations. Interestingly, the trend observed with respect to moderate acid sites was reverse and followed the trend as:  $\text{TMA} < \text{TEA} < \text{TPA}$ . Although, it is reported that [24], the

acidity decreases with increase in the copper content in  $\text{Cu}/\text{Al}_2\text{O}_3$  catalyst, in present studies, it may be attributed to the variation in the precipitating agent as there is no variation made in copper content.

### 3.3. Catalytic performance

#### 3.3.1. Influence of precipitating agents

The catalytic performance of r-CAR, r-URE and r-TMA in the dehydrogenation of cyclohexanol to cyclohexanone is depicted in Fig. 7. In the absence of catalyst, there was almost no cyclohexanol conversion at  $250^\circ\text{C}$ . However, under the identical set of reaction conditions, Alumina showed 10% cyclohexanol conversion with nearly 83.5% cyclohexene selectivity. The higher selectivity may be attributed to the acidity of alumina which is capable of dehydrating the cyclohexanol leading to the selective formation of cyclohexene [9–11,24].

Among r-CAR, r-URE and r-TMA, r-TMA showed the highest cyclohexanol conversion (69.6%) with 79.4% cyclohexanone selectivity. Probably, the higher conversion of cyclohexanol might be due to the high amount of readily reducible copper ions and copper cluster like species  $[\text{Cu-O-Cu}]_n$  [5]. The improved selectivity of cyclohexanone over r-TMA may be associated with combined effect of high BET surface area, low total acidity, small crystallite size and well dispersed copper. Probing further into the role of  $\text{Cu}^+$  and  $\text{Cu}^0$  species in controlling the selectivity of cyclohexanone, the catalytic activity of all the samples were compared as a function of  $\text{Cu}^+/\text{Cu}^0$  ratio (Table 1). Despite of lower  $\text{Cu}^+/\text{Cu}^0$  ratio, r-TMA exhibited highest cyclohexanone selectivity. This suggests that, not only XRD visible  $\text{Cu}^+$  species are responsible for higher selectivity of cyclohexanone, but also smaller crystallite site, lower total acidity,

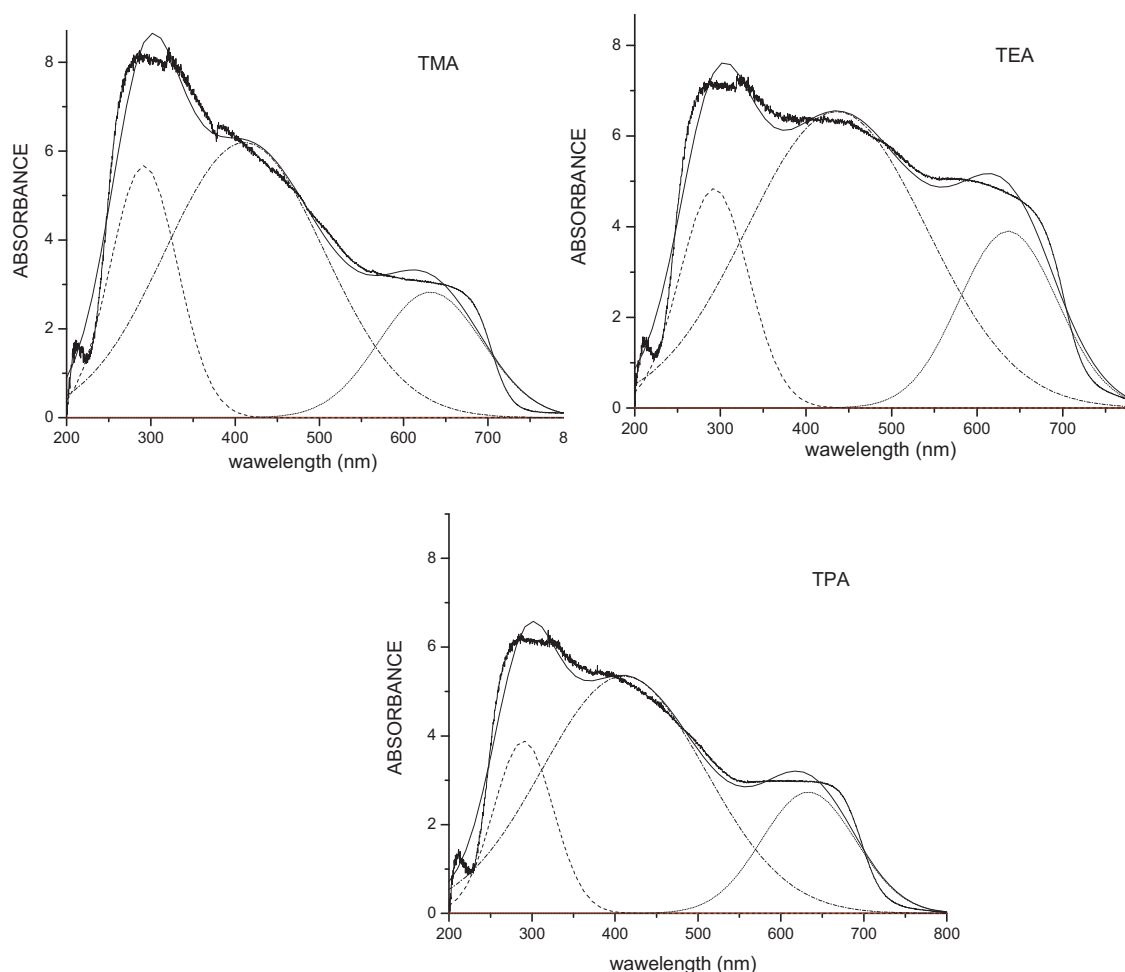


Fig. 5. DRUV-vis spectra of TMA, TEA and TPA.

higher surface area and possibly XRD invisible  $\text{Cu}^+$  species play an important role in enhancing the cyclohexanone selectivity. However higher selectivity of phenol over r-TMA might be due to the higher population of  $\text{Cu}^0$  species. In comparison with r-TMA, the r-URE showed lower cyclohexanol conversion on account of higher XRD visible  $\text{Cu}^+/\text{Cu}^0$  ratio, lowest surface area and higher copper crystallite size. The highest cyclohexene selectivity exhibited by r-CAR can be attributed to higher contribution of strong acidic

sites and total acidity. Moreover, it showed lower phenol selectivity due to higher XRD visible  $\text{Cu}^+/\text{Cu}^0$  ratio confirming lower  $\text{Cu}^0$  species [17]. Although the copper crystallite size of r-CAR was lowest among all, it showed 61.3% cyclohexanol conversion with 78.6% cyclohexanol and 19.3% cyclohexene selectivity which is in good agreement with reported literature [24]. Because of higher copper crystallite size and lower BET surface area, r-URE showed lower cyclohexanol conversion (42.1%) with 75.2% cyclohexanone selectivity. Thus, the overall performance of the catalyst in cyclohexanol dehydrogenation reaction is controlled by cumulative effect of its BET surface area, crystallite size, total acidity, distribution of acid sites, copper dispersion and bulk  $\text{Cu}^+/\text{Cu}^0$  ratio which, in turn, governed by judicious choice of the precipitating agent. In view of further improvement in the catalytic performance and to gain insight, catalyst prepared using TAAOH with different chain length of tetraalkyl ammonium cations were examined.

#### 3.4. Influence of chain length of tetraalkyl ammonium cation

The catalytic conversion of cyclohexanol and the product selectivity to cyclohexanone, cyclohexene and phenol over  $\text{Cu}/\text{Al}_2\text{O}_3$  catalyst prepared by using different tetraalkyl ammonium hydroxides as precipitating agent are shown in Fig. 8. In present study, r-TPA showed maximum conversion of cyclohexanol (81.5%) with 79.6% cyclohexanone selectivity. The catalyst, r-TEA, showed 78.9% cyclohexanol conversion with 79.2% cyclohexanone selectivity. As compared to both these catalysts, r-TMA showed the least cyclohexanone yield. Thus, the  $\text{Cu}/\text{Al}_2\text{O}_3$  catalyst prepared using

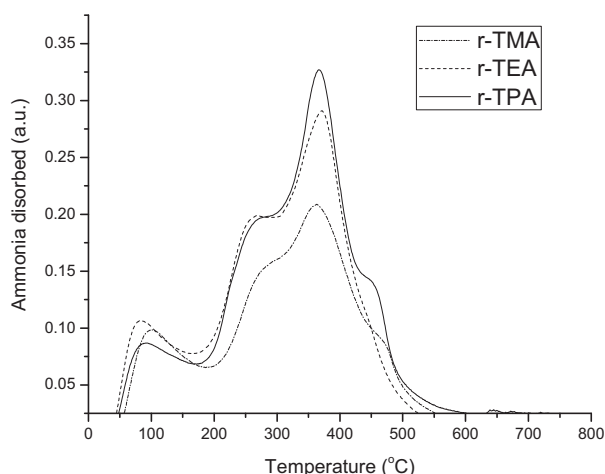
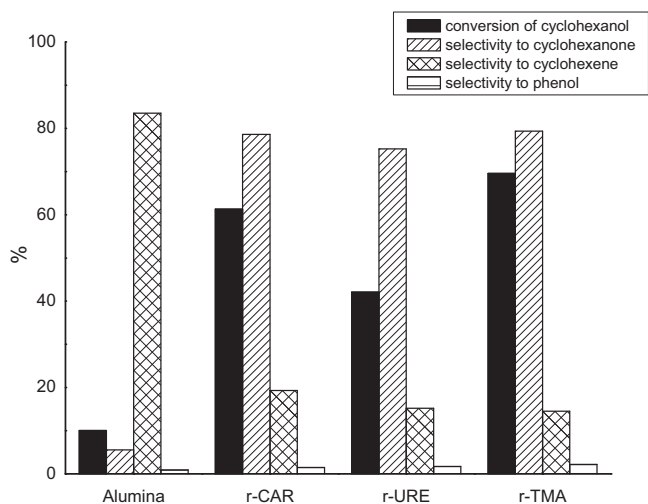
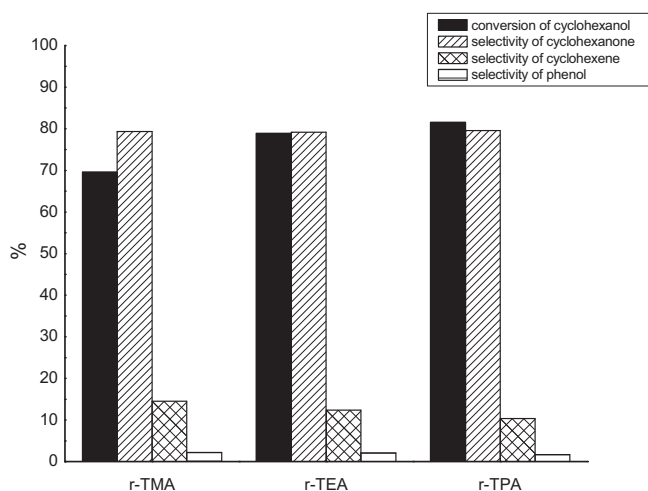


Fig. 6.  $\text{NH}_3$ -TPD profiles of r-TMA, r-TEA and r-TPA.



**Fig. 7.** Catalytic performance of Alumina and Cu/Al<sub>2</sub>O<sub>3</sub> catalysts prepared using different precipitating agents. (Reaction conditions: catalyst loading: 3 g, temperature: 250 °C, reaction time: 1 h, WHSV: 5.0 h<sup>-1</sup>, N<sub>2</sub> flow: 50 cm<sup>3</sup> min<sup>-1</sup>.)



**Fig. 8.** Catalytic activity and product distribution over Cu/Al<sub>2</sub>O<sub>3</sub> catalysts prepared using different tetraalkyl ammonium hydroxides as precipitant. (Reaction conditions: catalyst loading: 3 g, temperature: 250 °C, reaction time: 1 h, WHSV: 5.0 h<sup>-1</sup>, N<sub>2</sub> flow: 50 cm<sup>3</sup> min<sup>-1</sup>.)

longer chain length in tetraalkyl ammonium cation has shown enhanced catalytic performance. An increase in the chain length of tetraalkyl ammonium cation resulted in the improved catalytic performance in the order: r-TMA < r-TEA < r-TPA. Further the increase in chain length of organocation corresponded to the increased in the intermediate acidity per sq. meter of the catalysts. The enhancement of chain length in tetraalkyl ammonium cation may increase the degree of nucleation and the growth of new particle leads to increase in dispersion of copper which in the order TMA < TEA < TPA. The establishment of increasing trend of reducible copper cluster species [Cu-O-Cu]<sub>n</sub> facilitate the cyclohexanol conversion [5]. The optimum catalyst prepared by reduction of mixed oxide precursor synthesized using tetrapropyl ammonium hydroxide as precipitating agent, showed highest cyclohexanol conversion (81.5%) and cyclohexanone selectivity (79.6%) at 250 °C on account of higher Cu<sup>+</sup>/Cu<sup>0</sup> ratio, well dispersed copper, higher surface area and higher population of moderate acidic sites. It has shown 1.7% phenol selectivity.

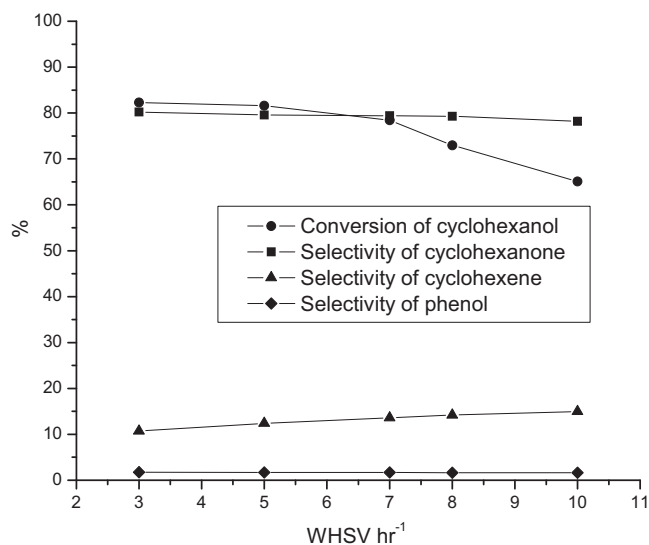


**Fig. 9.** Effect of contact time of r-TPA on conversion of cyclohexanol and selectivity to cyclohexanone, phenol, cyclohexene. (Reaction conditions: TPA catalyst loading: 3 g, temperature: 250 °C, reaction time: 1 h, N<sub>2</sub> flow: 50 cm<sup>3</sup> min<sup>-1</sup>.)

### 3.5. Influence of weight hourly space velocity (WHSV)

The effect of WHSV on the cyclohexanol conversion and the product selectivities over optimum catalyst (r-TPA) is illustrated in Fig. 9. It can be seen that, WHSV has an influence on the extent of formation of cyclohexanone, cyclohexene and phenol. The conversion of cyclohexanol to cyclohexanone was found to increase considerably from 65.0 to 81.5% without considerable change in the cyclohexanone selectivity when WHSV was decreased from 10 to 3 h<sup>-1</sup>.

## 4. Conclusions

Cu/Al<sub>2</sub>O<sub>3</sub> catalysts (molar Cu:Al = 1:1) were prepared by reduction of mixed oxide precursors synthesized using different precipitating agents viz. potassium carbonate, tetraalkyl ammonium hydroxides (TAAOHs) and urea. The degree of crystallinity and the magnitude of crystallite size of CuO in mixed oxide precursor were found to follow the trend as: CAR < TMA < URE. Compared to other two samples, the larger crystallite size of CuO in URE may be associated with higher rate of nucleation of primary particles and enhanced acceleration in the growth of primary particles. Although the samples were reduced under the identical conditions, Cu<sup>+</sup>/Cu<sup>0</sup> were found to vary with the variation in precipitating agent. The r-TMA catalyst prepared using tetramethyl ammonium hydroxide as precipitating agent was found to be potential catalyst for cyclohexanol dehydrogenation at lower temperature. The overall performance of the catalyst in cyclohexanol dehydrogenation reaction is controlled by cumulative effect of its BET surface area, crystallite size, total acidity, distribution of acid sites, copper dispersion and bulk Cu<sup>+</sup>/Cu<sup>0</sup> ratio which, in turn, governed by judicious choice of the precipitating agent. The increase in the chain length of tetraalkyl ammonium cation was found to improve further the catalytic performance in terms of cyclohexanol conversion in the order of r-TMA < r-TEA < r-TPA with similar selectivity to cyclohexanone. In present studies, at temperature 250 °C, after reduction of mixed oxide precursor synthesized using tetrapropyl ammonium hydroxide as precipitating agent, showed 81.5% cyclohexanol conversion and 79.6% selectivity. It can be concluded that, use of TAAOHs as precipitating agents resulted in the formation of catalyst with higher Cu<sup>+</sup>/Cu<sup>0</sup> ratio, well dispersed copper, higher surface area and lower total acidity with higher population of

moderate acidic sites which helped to maximize the yield of cyclohexanone by cyclohexanol dehydrogenation.

## Acknowledgements

The authors express their gratitude to Dr C.V. Rode and Dr. V.V. Bokade for helpful discussions and guidance. The assistance of Miss Sharda Kondawar in catalyst characterization, in particular to BET surface area and NH<sub>3</sub> TPD measurements is gratefully acknowledged.

## References

- [1] A. Romero, A. Santos, D. Escrig, E. Simon, *Appl. Catal. A: Gen.* 392 (2011) 19–27.
- [2] E. Simon, J.M. Rosas, A. Santos, A. Romero, *Catal. Today* 187 (2012) 150–158.
- [3] F.J. Brocker, M., Hesse, R. Markl, US Patent no. 6162758 (2000).
- [4] C.H. Sivaraj, P.K. Rao, *Appl. Catal.* 45 (1988) 103–114.
- [5] M. Popova, M. Dimitrov, V. Dal Santo, N. Ravasio, N. Scotti, *Catal. Commun.* 17 (2012) 150–153.
- [6] H.F. Chang, M.A. Saleque, W. Su Hsu, W.H. Lin, *J. Mol. Catal. A: Chem.* 109 (1996) 249–260.
- [7] H.F. Chang, M.A. Saleque, *Appl. Catal. A: Gen.* 103 (1993) 233–242.
- [8] C.H. Sivaraj, B.M. Reddy, P.K. Rao, *Appl. Catal.* 45 (1988) L11–L14.
- [9] F.M.T. Mendes, M. Schmal, *Appl. Catal. A: Gen.* 151 (1997) 393–408.
- [10] G.S. Jeon, G. Seo, J.S. Chung, *Korean J. Chem. Eng.* 13 (1996) 642–646.
- [11] G.S. Jeon, G. Seo, J.S. Chung, *Korean J. Chem. Eng.* 12 (1995) 132–133.
- [12] G.S. Jeon, G. Seo, J.S. Chung, *Korean J. Chem. Eng.* 13 (1996) 412–414.
- [13] G.S. Jeon, J.S. Chung, *Korean J. Chem. Eng.* 14 (1997) 49–58.
- [14] D. Ji, W. Zhu, Z. Wang, G. Wang, *Catal. Commun.* 8 (2007) 1891–1895.
- [15] G.K. Reddy, P.K. Rao, *Catal. Lett.* 45 (1997) 93–96.
- [16] Y.K. Vyawahare, V.R. Chumbhale, S.A. Pardhy, V. Samuel, A.S. Avsar, *Indian J. Chem. Technol.* 17 (2010) 43–49.
- [17] V.Z. Fridman, A.A. Davydov, *J. Catal.* 195 (2000) 20–30.
- [18] V.Z. Fridman, A.A. Davydov, K. Titievsky, *J. Catal.* 222 (2004) 545–557.
- [19] G. Ranga Rao, S.K. Meher, B.G. Mishra, P. Hari, K. Charan, *Catal. Today* 198 (2012) 140–147.
- [20] X. Li, B. Liang, J. Taiwan, *J. Taiwan Inst. Chem. Eng.* 43 (2012) 339–346.
- [21] A. Szegedi, M. Popova, K. Lazar, *React. Kinet. Mech. Catal.* 104 (2011) 291–301.
- [22] M. Popova, A. Szegedi, K. Lazar, A. Dimitrova, *Catal. Lett.* 9 (2011) 1288–1296.
- [23] G. Bai, H. Wang, H. Ning, F. He, G. Chen, *React. Kinet. Catal. Lett.* 94 (2008) 375–383.
- [24] C.H. Sivaraj, S.T. Srinivas, V.N. Rao, P.K. Rao, *J. Mol. Catal.* 60 (1990) L23–L28.
- [25] S. Nishimura, T. Shishido, K. Ebitani, K. Teramura, T. Tanaka, *Appl. Catal. A: Gen.* 378 (2010) 185–194.
- [26] M.W. Kasture, P.S. Niphadkar, N. Sharanappa, S.P. Mirajkar, V.V. Bokade, P.N. Joshi, *J. Catal.* 227 (2004) 375–383.
- [27] P.S. Niphadkar, P.N. Joshi, S.S. Deshpande, V.V. Bokade, *Appl. Catal. A: Gen.* 401 (2011) 236–240.
- [28] S.L. Burkett, M.E. Devis, *Chem. Mater.* 7 (1995) 920.
- [29] H. Bönemann, G. Braun, W. Brijoux, R. Brinkmann, A.S. Tilling, K. Seevogel, K. Siepen, *J. Organomet. Chem.* 520 (1996) 143.
- [30] M.D. Fokema, E. Chiu, J.Y. Ying, *Langmuir* 16 (2000) 3154–3159.
- [31] V.V. Paikar, P.S. Niphadkar, V.V. Bokade, P.N. Joshi, *J. Am. Ceram. Soc.* 90 (2007) 3009–3012.
- [32] J. Yang, S. Mei, J.M.F. Ferreira, *J. Am. Ceram. Soc.* 84 (2001) 1696–1702.
- [33] R.B. Mane, A.M. Hengne, A.A. Ghalwadkar, S. Vijayanand, P.H. Mohite, H.S. Potdar, C.V. Rode, *Catal. Lett.* 135 (2010) 141–147.
- [34] P.A. Kumar, M.P. Reddy, L.K. Ju, B.H. Sook, H.H. Phil, *J. Mol. Catal. A: Chem.* 291 (2008) 66–74.
- [35] A. Bialas, P. Niebryzdyowska, B. Dudek, Z. Piwowarska, L. Chmielarz, M. Michalik, M. Kozak, P. Kustrowski, *Catal. Today* 176 (2011) 413–416.
- [36] R.O. Idem, N. Bakshi, *Ind. Eng. Chem. Res.* 33 (1994) 2047.
- [37] M. Yin, C.K. Wu, Y. Lou, C. Burda, J.T. Koberstein, Y. Zhu, S. O'Brien, *J. Am. Chem. Soc.* 127 (2005) 9506–9511.
- [38] Y. Feng, H. Yin, L. Shen, A. Wang, Y. Shen, T. Jiang, *Chem. Eng. Technol.* 36 (2013) 73–82.
- [39] L. Chen, T. Horiuchi, T. Osaki, T. Mori, *Appl. Catal. B: Environ.* 23 (1999) 259–269.
- [40] M.C. Marion, E. Garbowski, M. Primet, *J. Chem. Soc. Faraday Trans.* 86 (1990) 3027–3032.
- [41] H. Praliaud, S. Mikhailenko, Z. Chajar, M. Primet, *Appl. Catal. B: Environ.* 16 (1998) 359–374.